2.6 INVESTIGATION OF 2-3 FEB 1998 CALIFORNIA EXTRATROPICAL STORM USING COAMPS^{TM}

Brian J. Gaudet and J.M. Schmidt *
Naval Research Laboratory – Monterey.

1. INTRODUCTION

During the 1997-1998 winter season, the California Land-Falling Jets Experiment (CALJET) was performed to study storm systems as they moved onshore, and in particular the importance of the low-level jet (LLJ) to the intense rain events that often accompany these systems (Ralph et al. 1999). In addition to conventional observational platforms in the region, the £eld project made use of NOAA P-3 aircraft ¤ight observations and dropsondes, and a set of 915 MHz coastal wind pro£lers. One well-observed event was that of 2-3 Feb 1998, which produced wind gusts of up to 40 m s^{-1} and as much as 300 mm of rain from the central California coast south, resulting in widespread ¤ooding and wind damage (Storm Data 1998; Persson et al. 1999b).

This paper will address the attempt to reproduce the complex frontal structure of this event using the Coupled Ocean/Atmosphere Mesoscale Prediction System (COAMPS^{TM}) model. As the system made landfall the interaction with the topography added a further complication to the structure. The numerical model incorporates the topographic in¤uence in the simulation, but the behavior of the system over land will not be a major focus of this paper.

2. MODEL

COAMPS^{TM} is a non-hydrostatic three-dimensional compressible model developed by the Naval Research Laboratory; the key features of the model design can be found in Hodur (1997). The microphysics scheme used in this version of the model is adapted from Rutledge and Hobbs (1983), and predicts the mixing ratios of cloud water, rain, pristine ice, and snow.

The simulation was run with four nested grids of grid spacings 81, 27, 9, and 3 km (Figure 1), and took its initial and boundary conditions from the Navy Operational Global Atmospheric Prediction System (NOGAPS) model and other data sources such as rawinsondes, ship observations, and satellites. A Multivariate Optimum Interpolation (MVOI) analysis is performed on the data along pressure levels (Barker 1992; Goerss and Phoebus 1992). The initialization time was 1200 UTC 01 Feb 1998, and the simulation was allowed to continue until 1200 UTC 03 Feb 1998 using a 12-hour data assimilation cycle.

*Corresponding author address: Brian J. Gaudet, Naval Research Laboratory – Monterey, 7 Grace Hopper Ave., Monterey, CA 93943; e-mail: gaudet@nrlmry.navy.mil.

3. SYSTEM OVERVIEW

During this period a deep low-pressure system was centered off the northern California coast, and the jet stream carried a series of disturbances forward and southward into California (Storm Data 1998). The model wind £eld at 500 m in Figure 2 for Grid 3 shows the main low off the northern California coast and a frontal zone near Pt. Conception at 0900 UTC on 3 Feb 1998. Figure 3 shows that the main randband is associated with both a jet streak left exit region and upper level dif¤uence.

Although the position of the frontal zone is well represented, the model is approximately £ve hours too fast with its timing (compare Persson et al. 1999b; Neiman et al. 2002). It is not known why this should be the case although resolution of the shortwave offshore is a possible explanation.

A number of narrow rainbands and frontal structures were observed with this system. The model frontal structure will be discussed in detail for Grid 4 in the next section. Although model precipitation forms near ridges inland and in the cold sector of the cyclone, the main frontal rainband is the only mesoscale-organized rainband apparent in the simulation. With a minimum grid spacing of 3 km, it is doubtful that the individual cells associated with the extensive convective rainfall associated with this event (Persson et al. 1999b; Neiman et al. 2002) can be adequately reproduced.

4. KINEMATICS OF FRONT

The 2-3 Feb 1998 system was observed by NOAA P-3 in cross-section as it made landfall over the southern California coast (Persson et al., 1999a,1999b). The observational cross-section showed a complex frontal structure, with essentially four zones of air (Figure 4.). Moving from east to west, ahead of the system there was a region of high equivalent potential temperature (θ_e) in southeasterly ¤ow, increasing to a maximum in a LLJ of approximately 30 m s^{-1}. Behind a very narrow transition zone was a region of southerly winds with reduced speeds and a 6 K reduction in θ_e. After approximately 140 km, there is a pool of slightly enhanced θ_e values. In another 40 km, θ_e gradually decreases again, achieving values well below those in the second region, and occurring in conjunction with northwesterly winds.

An offshore cross section through the model frontal region, despite some differences, does reproduce the gross features of the observed cross section (Figure 4.). For simplicity, the four main near-surface air masses from east to west will be referred to as the prefrontal region,

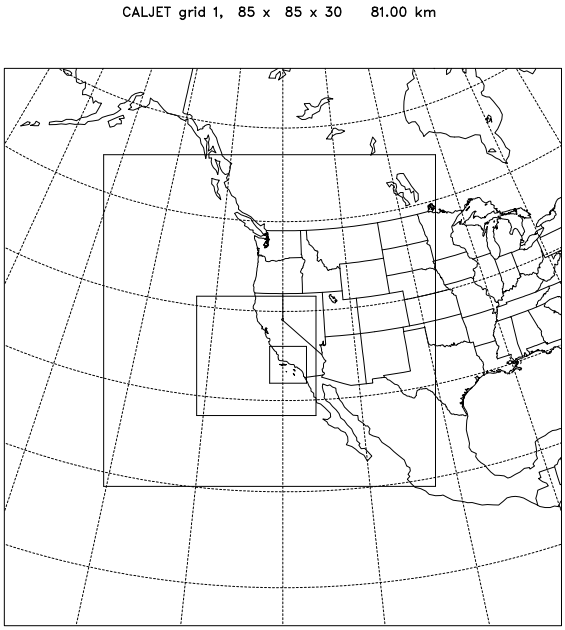

Figure 1: Model grids used in COAMPS^{TM} simulation.

cold pool, warm pool, and postfrontal region, respectively. The boundary between the cold pool and the prefrontal region seems to correspond to the primary cold front of Persson et al. (1999b), whereas the warm pool/postfrontal boundary resembles the secondary cold front. The cold pool appears to be an extension of the postfrontal region with storm-relative westerly momentum. (Equivalent potential temperature continues to decrease behind the secondary cold front but is not apparent in the color shading chosen for Figure 4..) The warm pool, as in the observations, is largely con£ned below 1 km, and contains storm-relative easterly ¤ow. The prefrontal region contains a LLJ whose maximum v-component speed of 28 m s^{-1} occurs just above the zone of highest θ_e (Figure 6) near 800 m. There is also an upper level v-jet associated with the blocking of the ambient ¤ow by the rainband to its east (Figure 7). Although there is some ambiguity in the tilt of the updraft, the core of highest θ_e tilts slightly forward (eastward) with height.

Well-de£ned horizontal wind shifts are apparent in regions approximately 140 km apart within approximately 1 km of the surface (Figure 8). These would correspond to the primary and secondary cold fronts of Persson et al. (1999b), and will be referred to as such in the model simulation for simplicity.

Trajectory analyses (Figures 8-9) show that parcels within the LLJ initially possess strong storm-relative westward momentum as they migrate rapidly northward. When they reach the rainband, however, they rapidly ascend within the updraft, encounter the strong westerly shear, and exit the storm to the east at high levels (5-7 km). Parcels above about 800 m never penetrate more than approximately 15 km westward of the primary front Parcels on the west side of the primary front arrive from the southwest. Those below approximately 1500 m subside as they pass along the front and eventually transition from storm-relative eastward ¤ow to storm-relative westward ¤ow[1]. These parcels are the primary constituents of the westward surging cold pool, although some near-surface (below 800 m) parcels from the prefrontal zone also move westward and downward through the precipitation into the cold pool.

The offshore LLJ shows a strong resemblance to the

[1]However, even when these parcels exhibit front-relative westward ¤ow, they are still predominantly moving eastward relative to the ground.

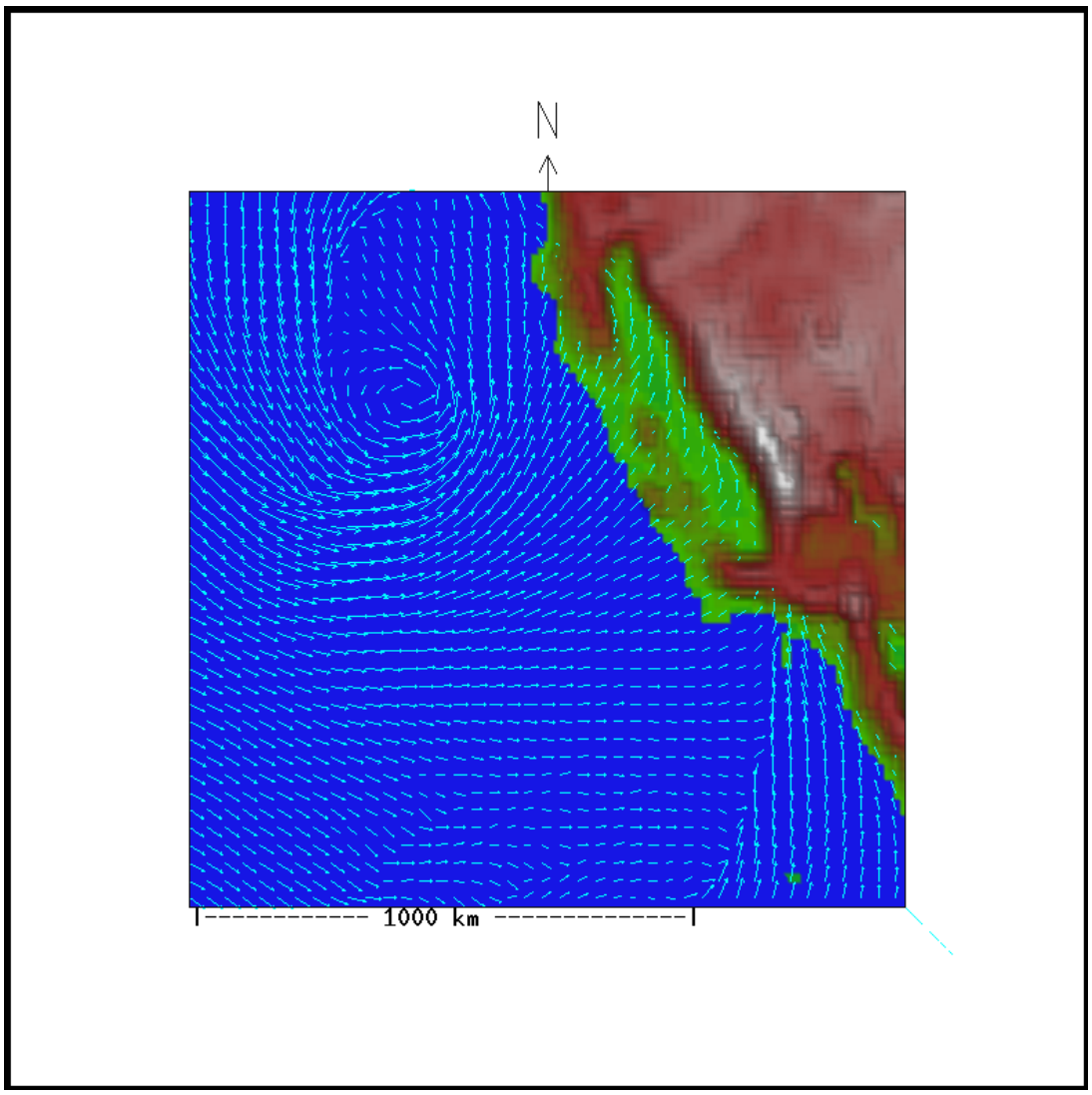

Figure 2: 500 m wind vectors at 0900 UTC 3 Feb 1998 for Grid 3 in simulation. California coast is to the upper right.

model proposed by Browning and Pardoe (1973) for an oceanic LLJ. First, the LLJ maximum is associated with and just to the east of a narrow band of high θ and θ_e air along the primary cold front. Browning and Pardoe proposed that the reversal of the normal temperature gradient along a cold front near the θ_e maximum causes a decrease in the geostrophic wind with height, leading to a maximum in the along-front wind at the base of the warm band (neglecting frictional effects). Second, backward trajectory analyses show that for a cross-section of the primary cold front region, the parcels that originate farthest to the south are those just to the east of the front (not shown). Browning and Pardoe proposed that the warm θ_e band can be explained in part because the parcels in the band originate the farthest to south due to the geometry of a developing baroclinic wave. Onshore, the LLJ rises relative to the surface and interacts with the topography in a complex manner.

Conceptually, the system shares some characteristics of both the forward-ascent and rearward-ascent cold front models of Browning (1986). At low-levels prefrontal trajectories possess enough storm-relative westward ¤ow to generate a line of precipitation and evaporatively cool the air behind. However, strong westerly shear at higher levels causes all prefrontal parcels originating above 1.5 km, and the more eastern regions of the LLJ, to remain forward of the storm.

To assess the impact of precipitation transport on the air masses, a simulation was performed in which cloud water and latent heating were allowed to occur, but the formation of other condensed water species was suppressed. A LLJ and primary frontal zone are still apparent, although there is a lag in the timing of the front (Figure 10). The major structural differences include the

absence of a near-surface low-θ_e zone immediately behind the primary cold front, which causes the associated low-level westward surge and secondary front to be less apparent kinematically. Another difference is that the LLJ is weaker and much more diffuse, suggesting that the precipitating system may act to focus the jet through convergence. The upper-level jet is also weaker and located well to the west of the primary front. The no precipitation simulation has a much wider condensate £eld and more front-to-rear ¤ow aloft, which could be attributed to the absence of the precipitation sink of latent heating (Figure 11).

5. CONCLUSION

The COAMPS^{TM} model has displayed skill in reproducing many of the quite complex features of the 2-3 Feb 1998 landfalling system, although admittedly de£cient in others. In particular, representations of many of the observed mesoscale rainbands and the widespread convection, both prefrontal and postfrontal, remain to be found. Increasing the horizontal resolution including more of the air-sea interaction associated with the anomalously-warm 1997-1998 SSTs should create a more realistic simulation. Tests with a new microphysics package that include the effects of graupel should are currently underway and should also greatly improve the model precipitation representation.

6. ACKNOWLEDGMENTS

We would like to thank Dr. Marty Ralph and Dr. Paul Neiman for generously giving us guidance and supplying us with data from the CALJET project. This work was supported in part by a grant of computer time from the Department of Defense High Performance Computing Modernization Program at the Army Research Laboratory Major Shared Resource Center in Aberdeen, MD. During this work the £rst author held a National Research Council Research Associateship Award at the Naval Research Laboratory in Monterey, CA.

REFERENCES

Barker, E., 1992: Design of the Navy's multivariate optimum interpolation analysis system. *Wea. Forecasting*, **7**, 220-231.

Browning, K.A., 1986: Conceptual models of precipitation systems. *Wea. Forecasting*, **1**, 23-41.

Browning, K.A., and C.W. Pardoe, 1973: Structure of low-level jet streams ahead of mid-latitude cold fronts. *Quart. J. Roy. Meteor. Soc.*, **99**, 619-638.

Goerss, J., and P. Phoebus, 1992: The Navy's operational atmospheric analysis. *Wea. Forecasting*, **7**, 232-249.

Hodur, R.M, 1997: The Naval Research Laboratory's Coupled Ocean/Atmosphere Mesoscale Prediction System (COAMPS). *Mon. Wea. Rev.*, **125**, 1414-1430.

Neiman, P.J., F.M. Ralph, A.B. White, D.E. Kingsmill, P.O.G. Persson, 2002: The statistical relationship between upslope ¤ow and rainfall in California's coastal mountains: Observations during CALJET. *Mon. Wea. Rev*, **130**, 1468-1492.

Persson, O., M. Ralph, B. Walter, P. Neiman, C. King, A. White, and J. Wilczak, 1999: Observations of the structure of the low-level jet in landfalling witner storms using the CALJET observational network. Preprints, *Third Symposium on Integrated Observing Systems*, Dallas, TX.

Persson, O., P. Neiman, M. Ralph, B. Walter, J.-W. Bao, S. Michelson, D. Jorgensen, and J. Schmidt, 1999: Measurements and modeling of air-sea interaction processes prior to heavy coastal precipitation: The case of Feb. 3, 1998. Preprints, *Third Conference on Coastal Atmospheric and Oceanic Prediction and Processes*, New Orleans, LA.

Ralph, F.M., P.O.G. Persson, D. Reynolds, W. Nuss, D. Miller, J. Schmidt, D. Jorgensen, J. Wilczak, P. Neiman, J.-W. Bao, D. Kingsmill, Z. Toth, C. Veldon, A. White, C. King, and J. Wurman, 1999: The California Land- falling Jets Experiment (CALJET): Objectives and design of a coastal atmosphere-ocean observing system deployed during a strong El Nino. *Preprints, 3rd Symp. on Integrated Observing Systems*, Dallas, TX.

Rutledge, S.A., and P.V. Hobbs, 1983: The mesoscale and microscale structure of organization of clouds and precipitation in midlatitude cyclones. VIII: A model for the "seeder-feeder" process in warm-frontal rainbands. *J. Atmos. Sci.*, **40**, 1185-1206.

Storm Data, 1998. National Oceanographic Atmsopheric Administration Environmental Data Series, **4**, Asheville, NC.

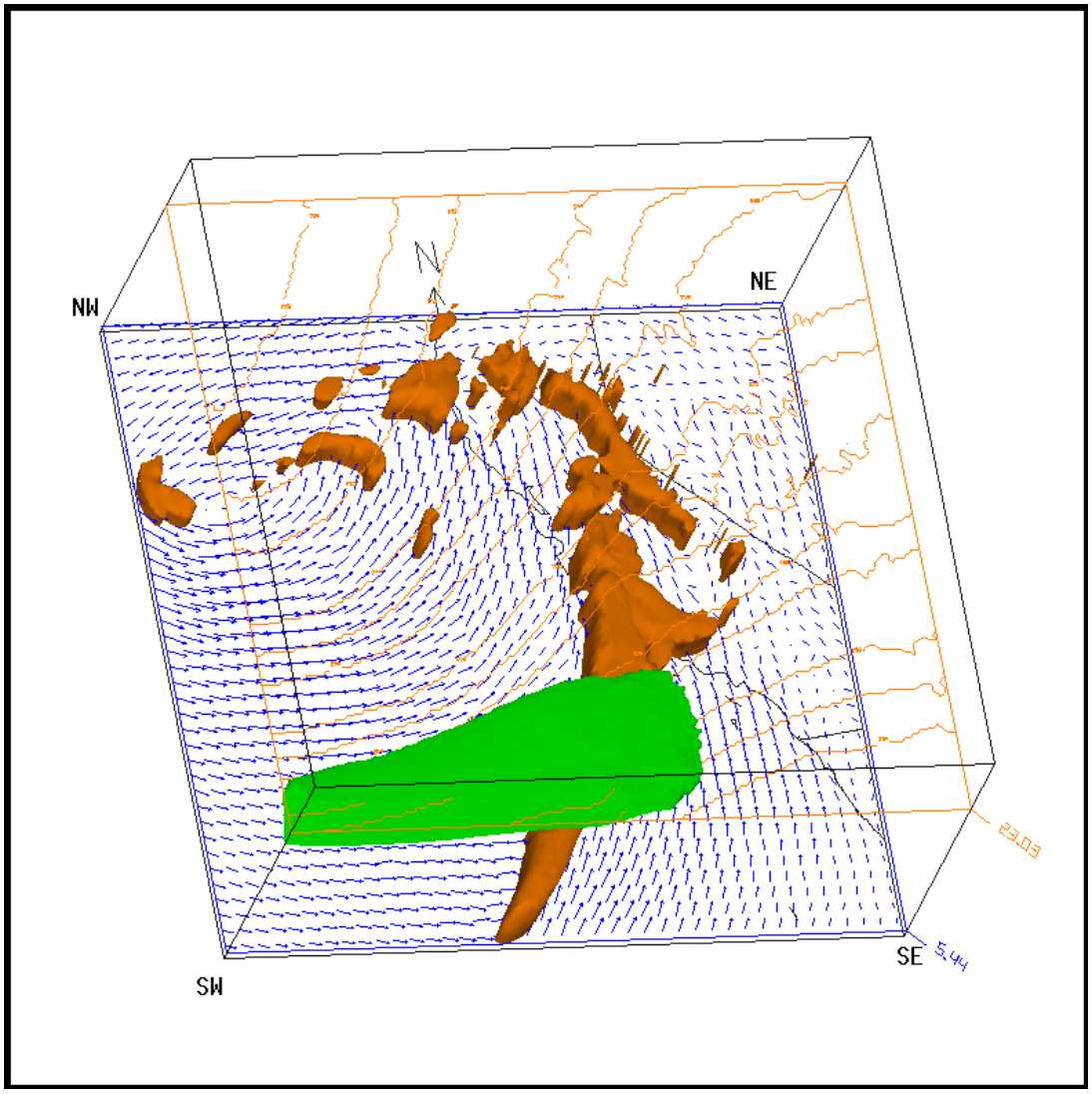

Figure 3: View from south-southwest of model Grid 3 at 0000 UTC 3 Feb 1998. Vectors show surface-relative wind velocity at 500 m. Green shading denotes wind speed greater than 85 m s^{-1}; orange shading denotes rain mixing ratio greater than 0.2 g kg^{-1}. Contours show pressure every 2 mb at 11 km.

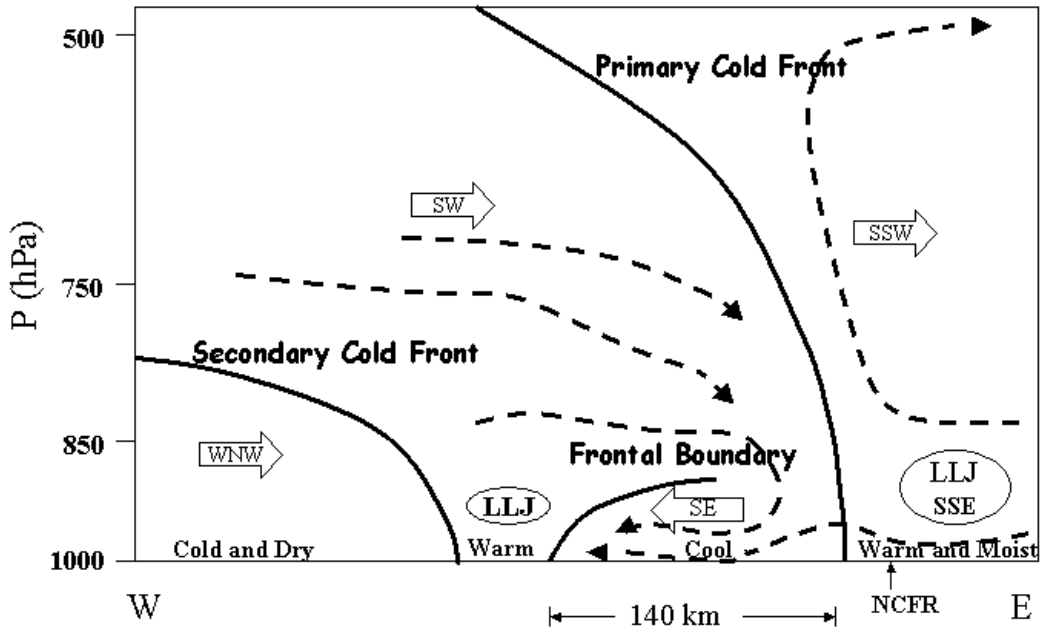

Figure 4: Schematic of cross-section through frontal zones. Scales, bold features, and block arrows correspond to those of observed 1300-1600 UTC 3 Feb 1998 cross-section, adapted from Persson et al. (1999b). Dashed lines correspond to storm-relative motion in modeled frontal system of current study.

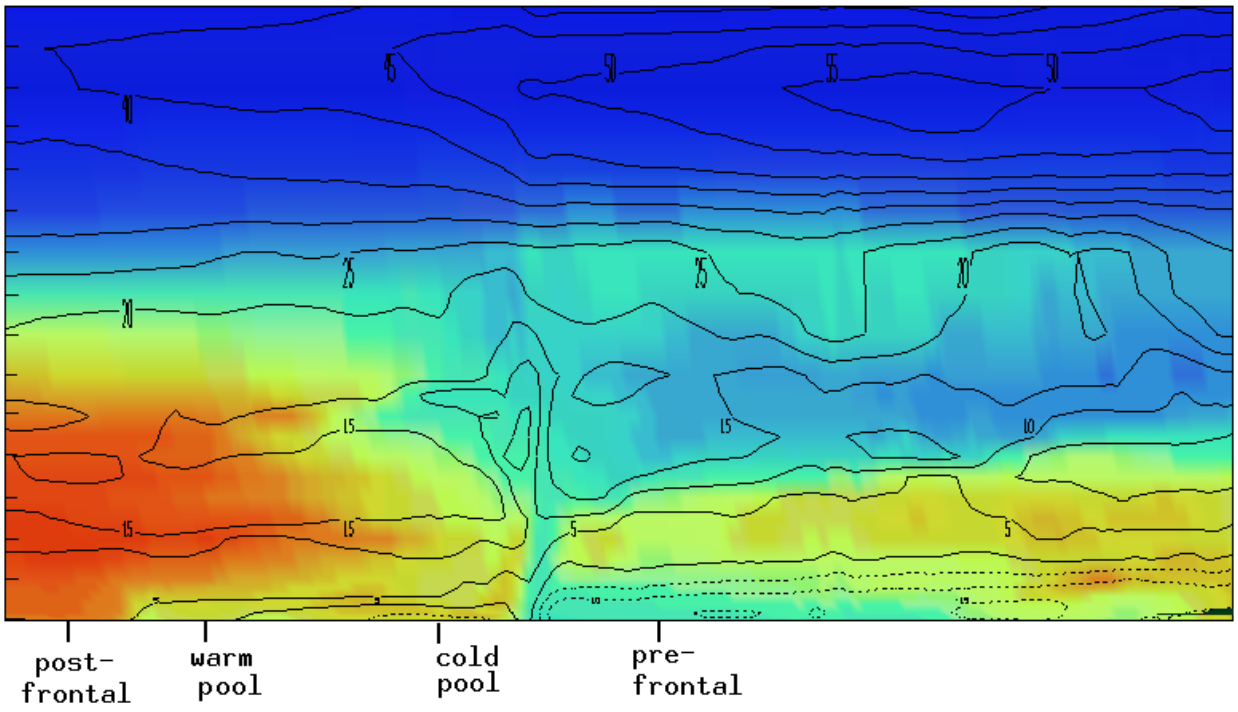

Figure 5: Cross-section through model Grid 4 for 32.8° N at 0800 UTC 3 Feb 1998. Color represents θ_e: orange, $\theta_e < 307$ K; yellow $\theta_e = 313$ K; green, $\theta_e = 317$ K; light blue, 320 K; blue, $\theta_e > 330$ K. Contours indicate storm-relative u-speed assuming storm u-speed of 7 m s^{-1}. Domain is 450 km across. Tick marks at left are separated by 1 km.

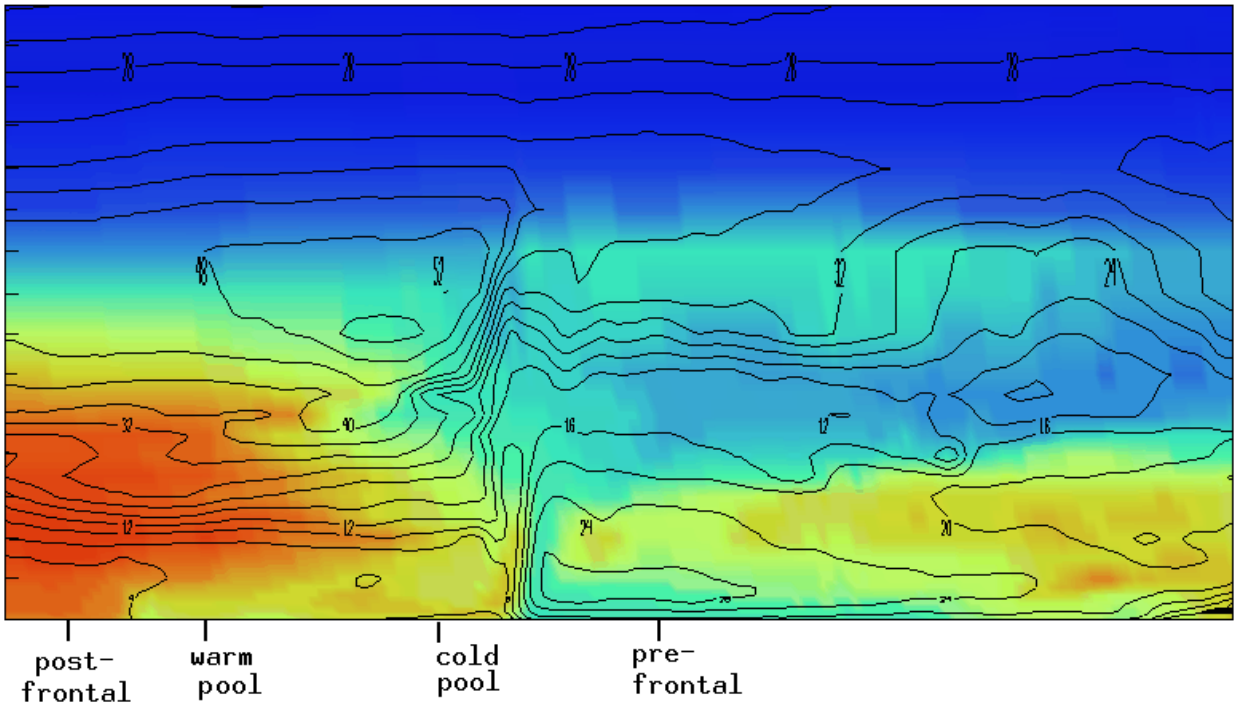

Figure 6: Same as Figure 4., but with contours indicating v-speed.

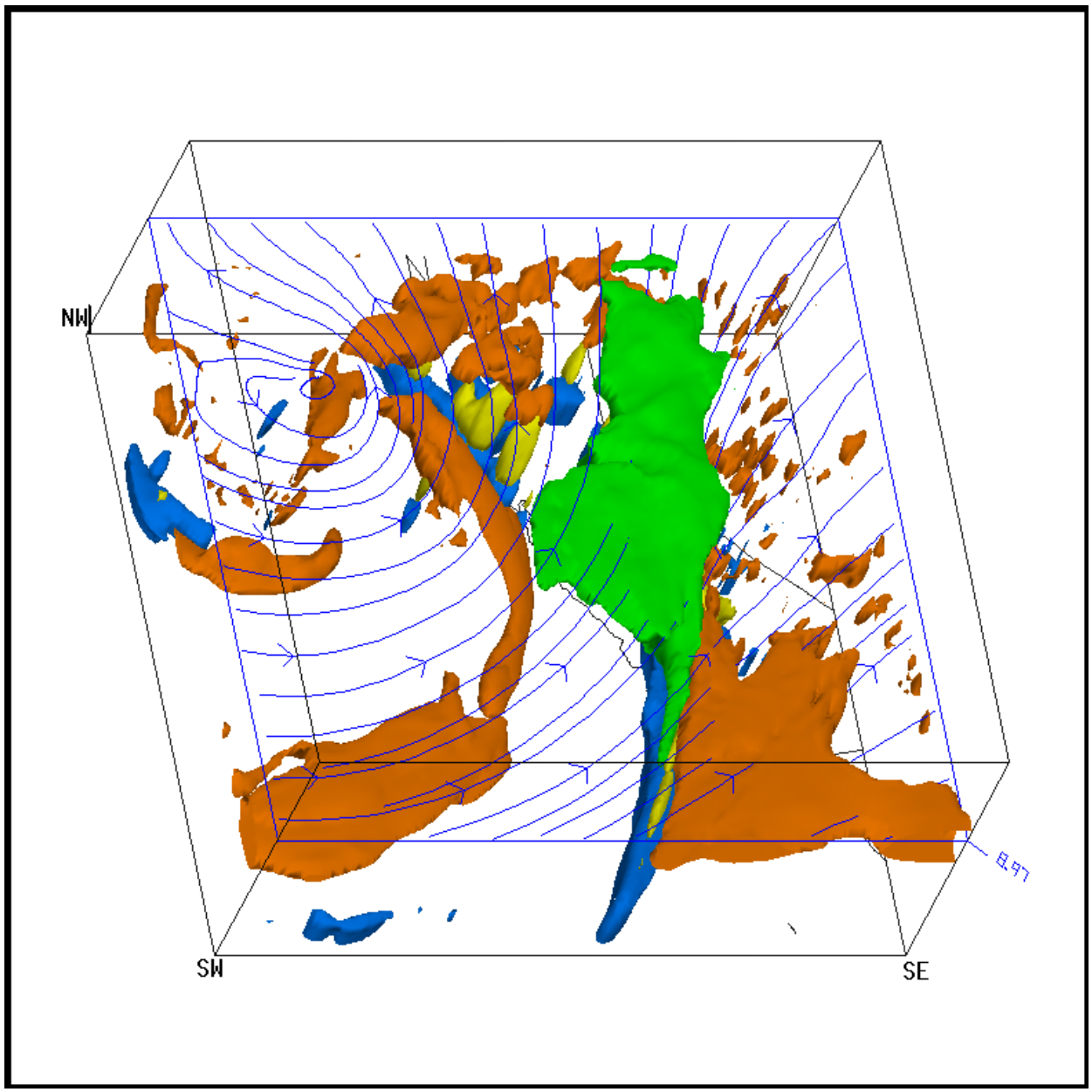

Figure 7: View from southwest of Grid 3 at 0400 UTC 3 Feb 1998. Streamlines show surface-relative velocity at 9 km. Green indicates $v > 45$ m s^{-1}; blue, orange, and yellow indicate rain, ice, and snow mixing ratios greater than 0.20, 0.10, and 0.20 g kg^{-1}.

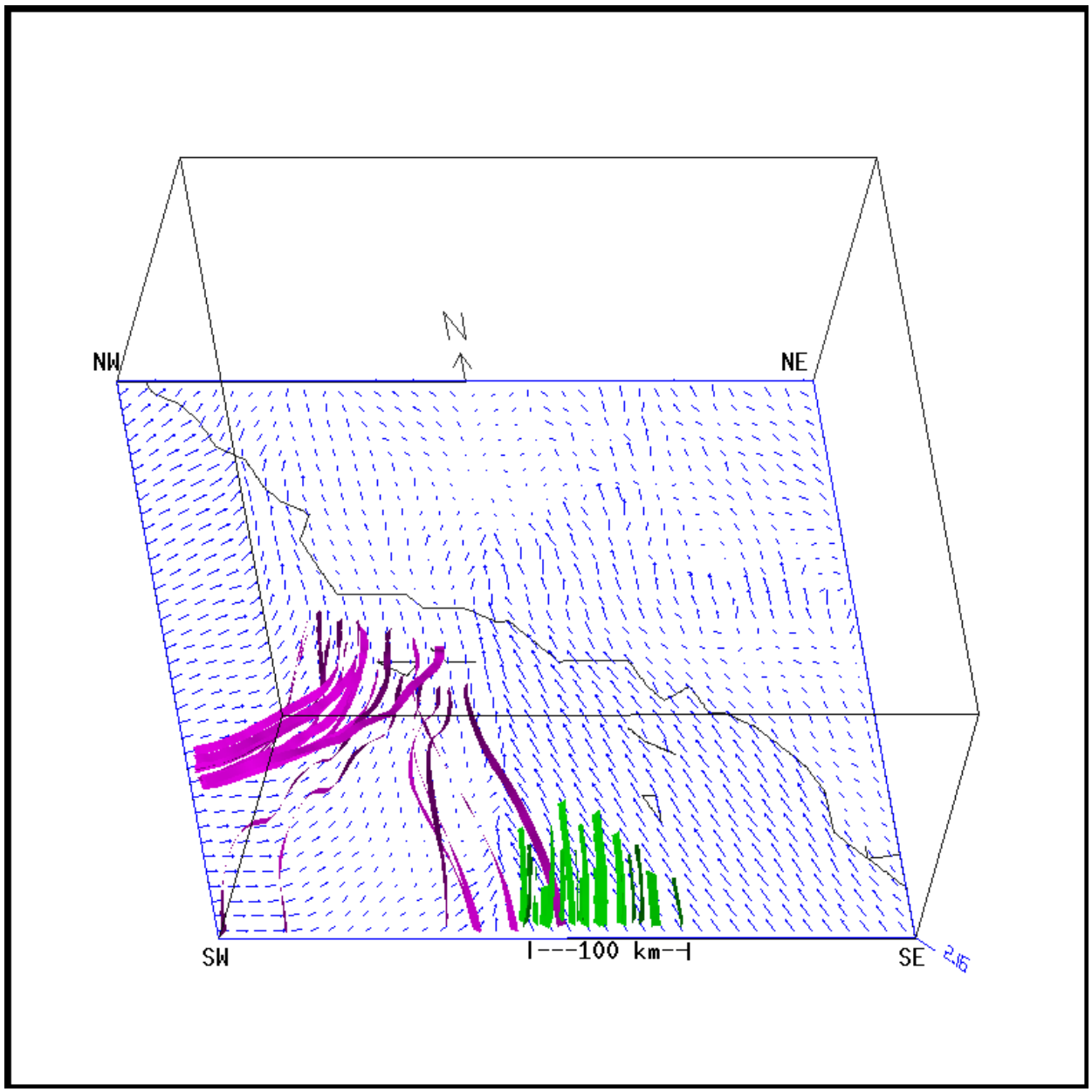

Figure 8: Grid 4 ground-relative wind vectors at 100 m above surface for 0600 UTC 3 Feb 1998, and trajectories from 0000-0600 UTC. Trajectory locations at 0600 UTC are 100 m above surface between fronts (magenta), and 800 m above surface near LLJ (green). View is from south-southwest.

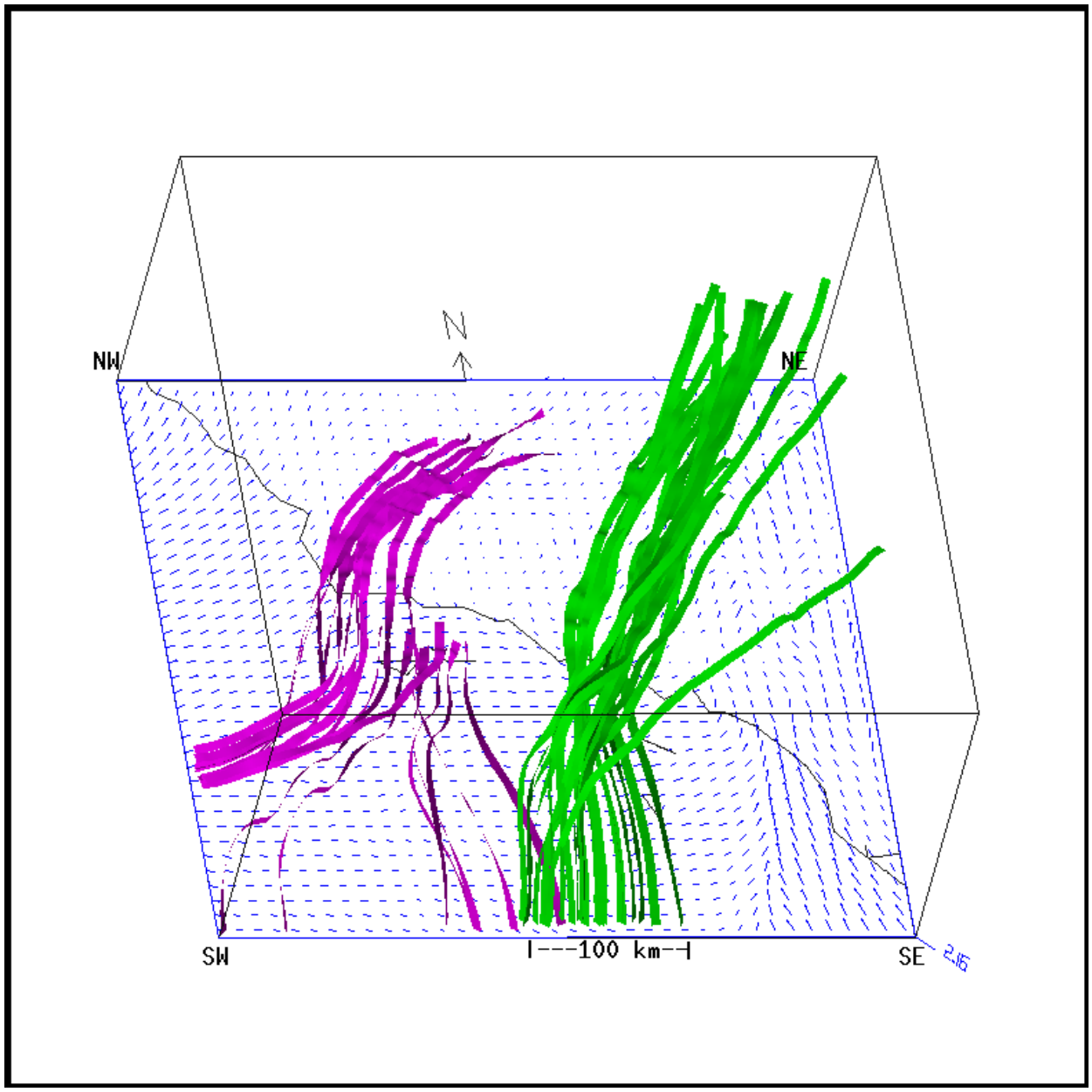

Figure 9: Same as 8, but showing trajectory positions and wind vectors for 1200 UTC.

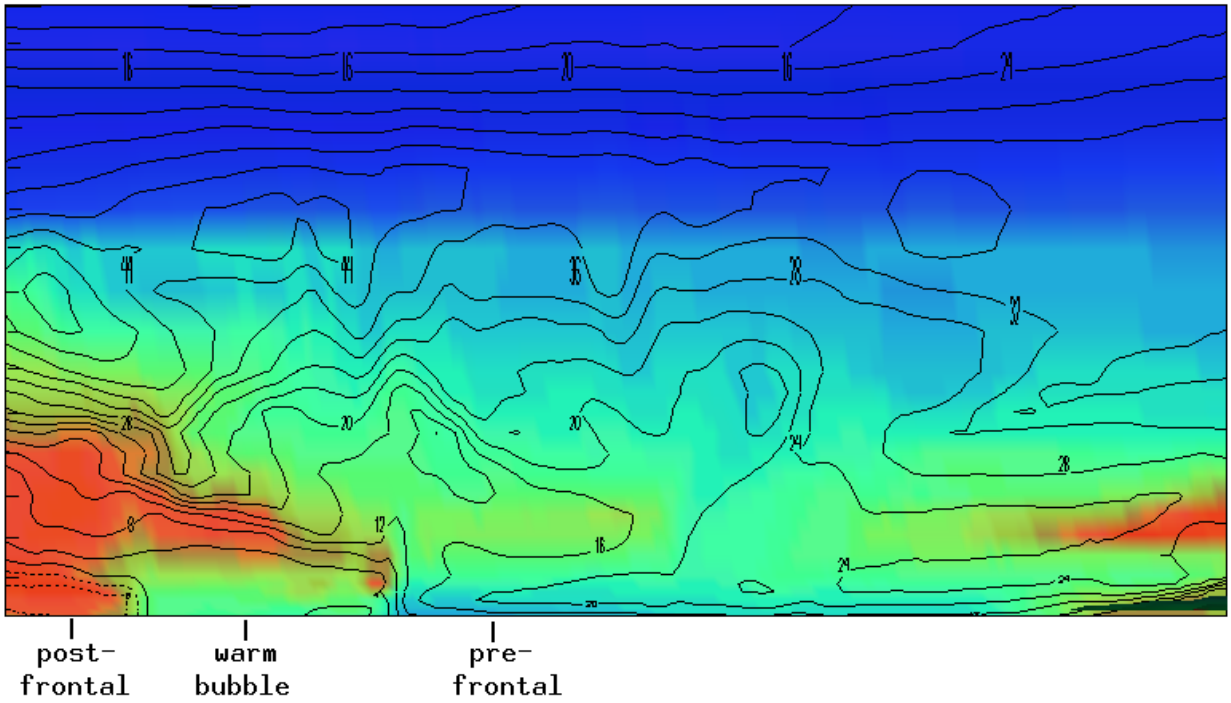

Figure 10: Same as 6, but for the no-precipitation run, near 33.2° N, at 1200 UTC 3 Feb 1998.

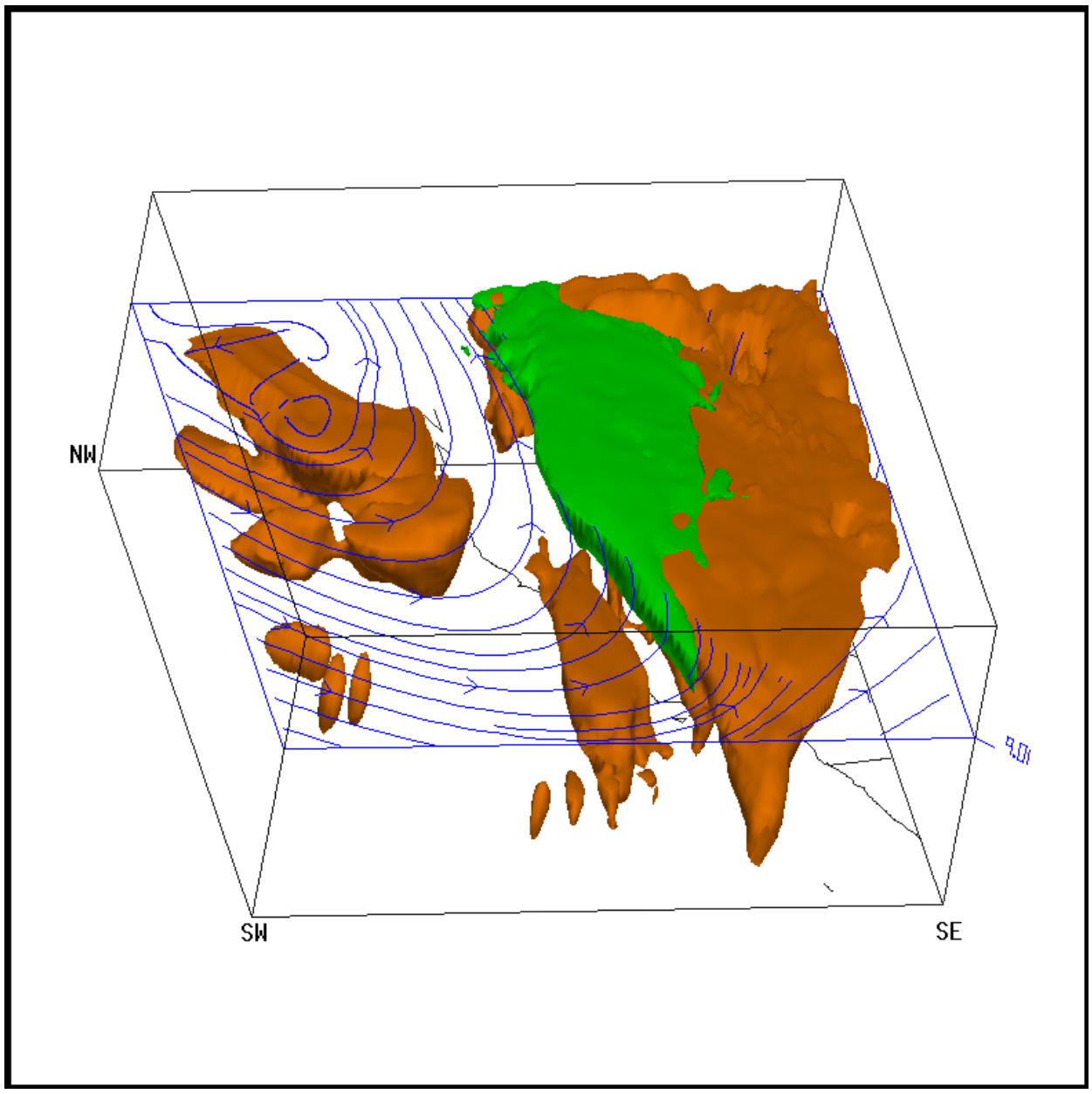

Figure 11: View from southwest of Grid 3 at 1200 UTC 3 Feb 1998 for no precipitation run. Streamlines show surface-relative velocity at 9 km. Green indicates $v > 45$ m s^{-1}; orange represents cloud water mixing ratio greater than 2.5 g kg^{-1}.